nature physics

Article

https://doi.org/10.1038/s41567-024-02456-6

Distinct elastic properties and their origins in glasses and gels

In the format provided by the authors and unedited

Supplementary Notes

Simulation methods for 2D glasses with the harmonic potential.

We conducted molecular dynamics simulations on a 2D binary mixture of particles interacting with harmonic potentials in a square box under the NVT ensemble with a Nose-Hoover thermostat. The pairwise potential $u(r_{ij})$ between particles i and j is described by a harmonic function:

$$u(r_{ij}) = \frac{\epsilon}{2}\left(1 - \frac{r_{ij}}{d_{ij}}\right)^2, \quad r_{ij} < d_{ij}, \tag{1}$$

where r_{ij} is the distance between particles i and j, and d_{ij} is the sum of their radii.

The system comprises $N = 4096$ particles, with an equal number of large and small particles and a diameter ratio of 1.4. The diameter d_s of the small particles is set as the length unit, and both the small and large particles possess the same mass m. The energy, time, and temperature are scaled in units of ϵ, $\sqrt{md_\mathrm{s}^2/\epsilon}$, and $10^{-3}\epsilon/k_\mathrm{B}$, respectively, where k_B represents the Boltzmann constant. The packing fraction of the system is fixed at $\phi = 0.91$.

Prior studies have thoroughly investigated the glassy dynamics of these glass formers [30,55,56]. The onset temperature T_on is approximately 2.1, the mode-coupling-theory (MCT) temperature T_mct is around 1.21, and the ideal glass transition temperature T_0 is roughly 0.63. In this study, we first equilibrated the system at $T = 3.0$ and then rapidly quenched it to $T = 1.0$ to observe the system's relaxation.

A total of 504 independent trajectories were performed for our investigation.

The thermal elastic moduli are measured via stress fluctuations and the athermal elastic moduli are measured via Hessian matrix, see Methods section.

Supplementary Figures

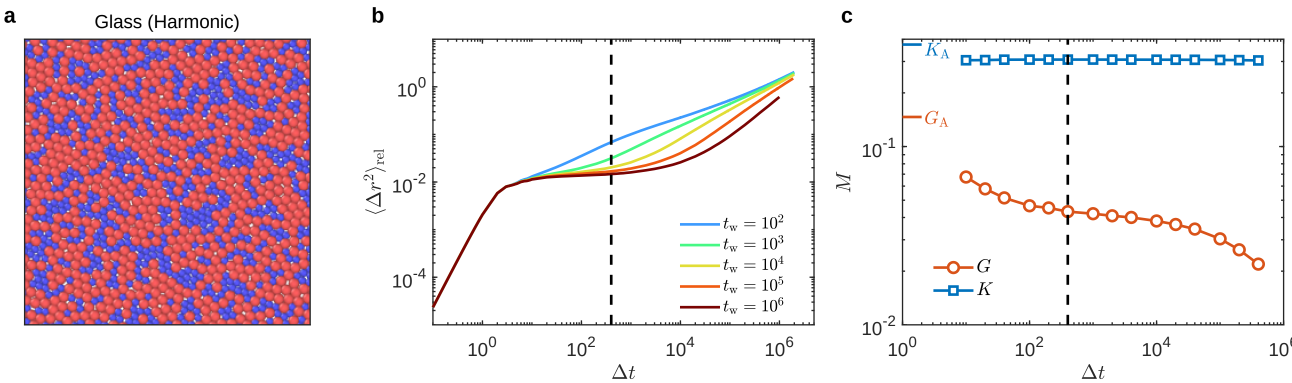

Supplementary Fig. 1. **Ageing dynamics and observation-time-dependent elasticity in glasses with the harmonic potential (harmonic glasses).** **a**, Illustration of the typical structure of a harmonic glasses. Particles are colour-coded based on their sizes. **b**, Cage-relative MSD $\langle \Delta r^2 \rangle_{\rm rel}$ versus observation time Δt at different ageing time, $t_{\rm w}$. **c**, Observation-time-dependent shear modulus G and bulk modulus K. Short bars indicate the affine moduli, $G_{\rm A}$ and $K_{\rm A}$. The same plot as the Fig. 1 in the main text.

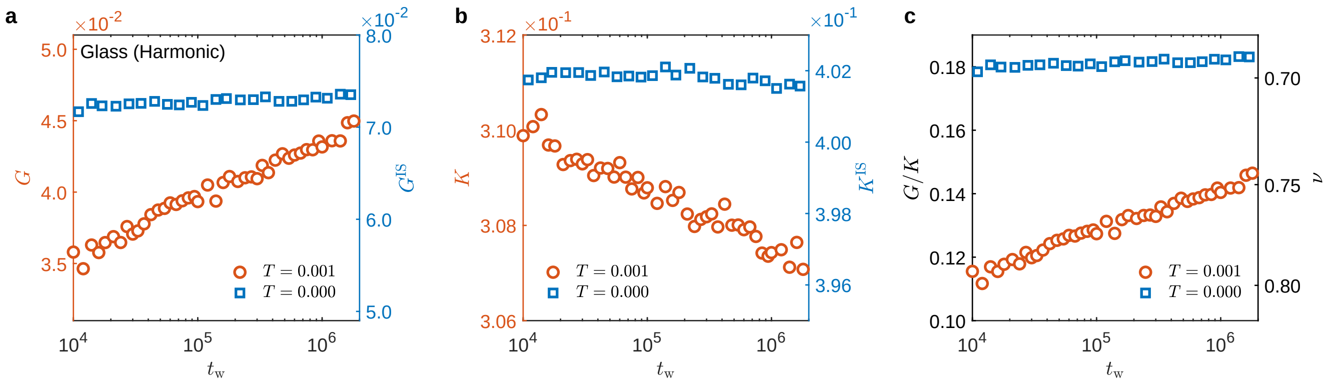

Supplementary Fig. 2. **Age-dependent elasticity in harmonic glasses.** The age-dependent thermal elasticity G (**a**), K (**b**), modulus ratio G/K and Poisson ratio ν (**c**) (red circles) and corresponding inherent elasticity at zero temperature (blue squares). The observation time Δt used to measure these moduli are marked by the vertical dashed lines in Supplementary Fig. 1. The same plot as the Fig. 2 in the main text.

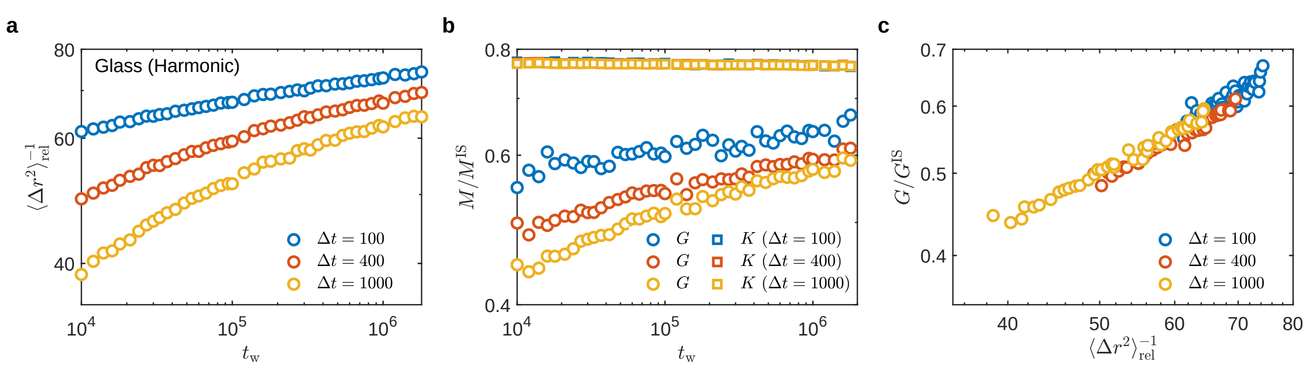

Supplementary Fig. 3. **Role of inherent elasticity and MSD on thermal elasticity in harmonic glasses.** **a**, Inverse of the cage-relative MSD $\langle \Delta r^2 \rangle_{\mathrm{rel}}^{-1}$ at different observation times Δt plotted against waiting time t_{w}. **b**, The ratios between thermal elasticity and inherent elasticity M/M^{IS} versus t_{w} for different Δt. **c**, The scaled shear modulus G/G^{IS} versus $\langle \Delta r^2 \rangle_{\mathrm{rel}}^{-1}$ for different Δt. The same plot as the Fig. 3 in the main text.

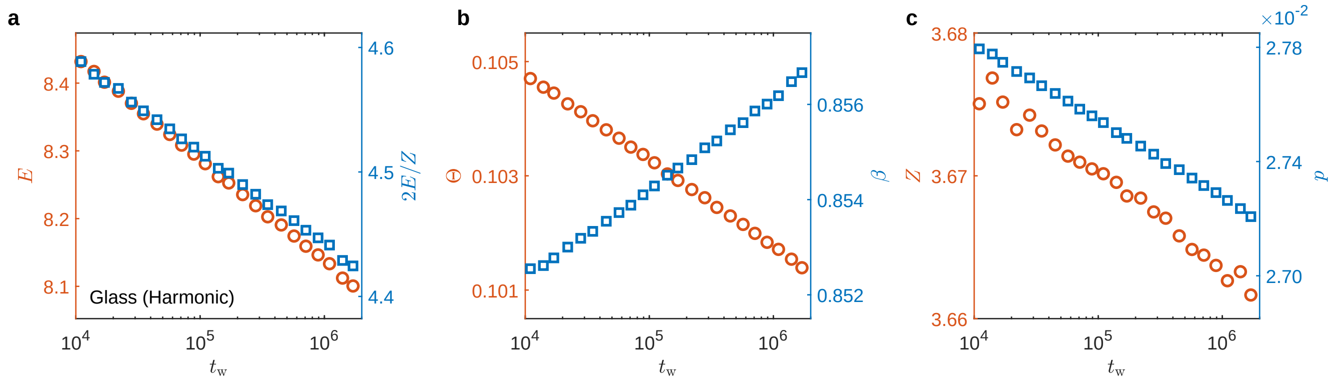

Supplementary Fig. 4. **Age-dependent potential energy and structure in harmonic glasses.** **a**, Age-dependent potential energy per particle (red open circles), E, and per contact (blue open squares), $2E/Z$. **b**, Age-dependent orientational order parameter Θ and anisotropy parameter η of Voronoi cells, where $\Theta = 0$ indicates perfect order and $\eta = 1$ indicates isotropic cells. **c**, Age-dependent contact number Z and pressure p. The same plot as the Fig. 4 in the main text.